

# PATHOLOGIC ANGIOGENESIS IN THE BONE MARROW OF HUMANIZED SICKLE CELL MICE IS REVERSIBLE BY BLOOD TRANSFUSION

Park, S.-Y. et al.

## SUPPLEMENTAL DATA

### Supplemental Methods

**Mouse model and study design** For the reconstitution of AA or SS mouse BM cells, we used 8 week old C57BL/6 wild type (WT) and CXCL12-GFP<sup>+</sup> reporter mice after 2 split-doses of whole-body irradiation (total 11 Gy) to generate chimera mice with SCD phenotype (SS → WT and SS → CXCL12-GFP<sup>+</sup> SCD mice; AA → WT and AA → CXCL12-GFP<sup>+</sup> control mice). CXCL12-GFP<sup>+</sup> knock-in, CXCL12-expressing cell reporter mice in which green fluorescent protein was knocked into the *Cxcl12* locus, were previously reported by Ara *et al.*<sup>1</sup> CXCL12-GFP<sup>+</sup> mice contain reticular niche cells that express high amounts of CXCL12 throughout the medullary bone marrow cavity, called CXCL12-abundant reticulocytes (CAR), often found in perivascular location.<sup>2</sup> All control mice were age- and sex- matched to the experimental mice. The animal protocol was approved by the Animal Care and Use Committee of the University of Verona (CIRSAL), the Boston Children's Hospital Animal Care and Use Committee, and the Institutional Animal Care and Use Committee at Massachusetts General Hospital. The sample size was estimated based on previous studies using humanized SCD mice.<sup>3</sup> For quantitative imaging analysis by LaSC scanning and 3D confocal, based preliminary analysis of BM vascular defects in SCD mice, power analysis was performed using PASS software (Version 15.0, NCSS), producing a report that group sample sizes of 4 have 90% power to reject the null hypothesis of equal means when the population mean difference is 30.0 with a standard deviation for both groups of 10.0 and with a significance level (alpha) of 0.05 using a two-sided two-sample equal-variance t-test. Animals were anesthetized with isoflurane, and randomly assigned to experimental groups. Whole blood was collected from each mouse via retro-orbital venipuncture by heparinized microcapillaries. BM exudate was collected as previously reported.<sup>4,5</sup> A 6 week transfusion regimen was carried as previously described with minor changes.<sup>6</sup> Briefly, sickle cell mice were transfused weekly with PBS-washed AA red cells (Hct 45%, two doses of 400  $\mu$ l/mouse with a 12 h interval) for 6 weeks. This strategy is based on the

low sickle red cell survival in the peripheral circulation (SS T50 = 3.5±0.4 days vs AA T50 = 18±2.1 days, p<0.02). Tail vein was used as the route of injection. Hematologic parameters and HPLC were carried at baseline and at 3 and 6 weeks of treatment. Hematological parameters and reticulocyte count were evaluated at baseline and at different time points as previously reported.<sup>7,8</sup> HbS levels were determined by high performance liquid chromatography (HPLC). The analysis of erythropoiesis, ROS and the amount of Annexin-V<sup>+</sup> erythroblasts was determined as previously described.<sup>9,10</sup> Follow-up of mouse spleen dimension was carried out by abdominal ultrasonography using VeVO 2100 high frequency ultrasound system (Fujifilm VisualSonics Inc., Canada).

**Mouse PCR genotyping and SS mouse phenotyping** CXCL12-GFP genotyping was performed using PCR primers (forward 5'- CTA GGC CAC AGA ATT GAA AGA TCT -3', reverse 5'- GTA GGT GGA AAT TCT AGC ATC ATC C -3') with the following condition: 95°C for 3 min; 34 cycles of 95°C for 15 s, 61°C for 15 s, and 72°C for 15 s, followed by 72°C for 10 min, 4°C forever, resulting in a 200-bp product. SCD mouse genotyping was performed according to Jackson Laboratory instruction. Briefly, hemoglobin S gene (human sickle hemoglobin beta,  $\beta^S$ ) and A gene (human wildtype hemoglobin beta,  $\beta^A$ ) were assessed by PCR with primers 1, 2, and 3 as described below: primer P1 (mouse beta KI forward) 5'-TTG AGC AAT GTG GAC AGA GAA GG -3', primer P2 (Beta A reverse) 5'- GTT TAG CCA GGG ACC GTT TCA G -3', and primer P3 (Beta S reverse) 5'-AAT TCT GGC TTA TCG GAG GCA AG -3' with the following condition (95°C for 3 min; 34 cycles of 95°C for 15 s, 61°C for 15 s, and 72°C for 15 s, and then following with 72°C for 10 min, 4°C forever). The amplified PCR products consist of 250-bp S gene product by P1 and P3 primers and 320-bp A gene product by P1 and P2 primers. Homozygous SS mice were confirmed by phenotyping splenomegaly and anemia by CBC analysis. We also performed HbS phenotype of SS mice by HPLC as shown in Figure 5B and 6D. We used only homozygous sickle mice (SS), not heterozygous mice (SA).

**Flow cytometry analysis** Single-cell BM suspensions were prepared by crushing and gently grinding the femurs and tibiae using a mortar and a pestle in washing buffer (Dulbecco's PBS [D-PBS], Ca<sup>2+</sup> free, Mg<sup>2+</sup> free, 2% FBS) followed by hemolysis with ammonium chloride-potassium buffer (Life Technologies BRL). Single-cell spleen suspensions and peripheral blood (PB) cells harvested by heart bleeding were washed with washing buffer and then hemolysis with ammonium chloride-potassium buffer. After blocking FcRs with anti-CD16/CD32 (2.4G2) Ab, cells were stained with specific Abs. The following Abs were purchased from eBioscience, and/or BioLegend: FITC-, PE-, APC-, PE-Cy7-, APC-Cy7, PerCP- labeled anti-B220 (RA3-6B2), anti-CD19 (6D5), anti-CD11b/ Mac-1 (M1/70), anti-Gr-1 (RB6-8C5), anti-CD3e (145-2C11), anti-CD4 (GK1.5), anti-CD8 (53-6.7), anti-Ter119 (TER119), anti-CD5 (53-7.3), anti-CD117/c-Kit (2B8), anti-CD34 (RAM 34), anti-CD16/32 (clone 93), anti-CD150 (TC15-12F12.2), anti-CD48 (HM48.1), anti-Sca-1 (D7), anti-CD135 (A2F10), anti-CD71 (RI7217), anti-CD45 (30-F11). Flow cytometric data was acquired by FACS Canto II (Becton Dickinson; 2-lasers with 8 parameters) or Attune NxT (Thermo Fisher; 4-lasers with 16 parameters), followed by flow cytometry analysis using the FlowJo Software (v10.6; BD).

**Colony-forming cell assay** *In vitro* colony-forming unit (CFU) assay of hematopoietic progenitor cells was performed using MethoCult™ (M3434, Stem Cell Technology) according to the manufacturer's instructions. Mononuclear cells (MNCs) were prepared from peripheral blood (PB) of 8 week old AA or SS mice. After calculating the blood volume of AA mice corresponding to 2 x 10<sup>5</sup> MNCs, MNCs from the equal volume of AA and SS mouse blood were plated per 35 mm petri dish. After 7-10 days of incubation in hypoxia workstation (Ruskin Invivo2 400; 3% O<sub>2</sub>), numbers of CFUs each plate were scored. The types of colonies (CFU-GEMM, CFU-G, CFU-M, CFU-GM, and BFU-E) were identified by the morphology of colonies according to manufacturer's instruction

### **Immunoblot analyses**

**Bone marrow cells and bone marrow exudate** To prepare enriched BM niche cells, i.e. mesenchymal stromal cells and vascular cells, crushed bones from mouse hind limbs were flushed with D-PBS (2% FBS) to remove suspended BM cells, followed by

incubation with collagenase IV and DNase I to suspend and harvest enriched BM niche cells according to Houlihan et al.<sup>11</sup> Ten million digested BM cells were collected and lysed by ultrasonication for 30 seconds (6 x 5 s). **Lysates of lung, liver, and heart cells.** Frozen lungs from each studied group were homogenized and lysed with iced lyses buffer (LB containing: 25 mM Bicine, Triton X-100 1.5%, EDTA 1 mM, NaF 1 mM, protease inhibitor cocktail tablets (Roche), 1 mM Na<sub>3</sub>VO<sub>4</sub> final concentration) then centrifuged 30 min at 4 °C at 12,000g. **Electrophoresis and immunoblot analyses.** Proteins were quantified using the BCA protein assay kit (Thermo Fisher) separated by 4-12% SDS-PAGE and transferred into PVDF membrane. After incubation with 5% BSA in TBST for 1 h at room temperature, the membrane was incubated with primary antibodies against target proteins at 4°C for overnight. Then, membrane was incubated with HRP-conjugated secondary antibodies (R&D, #HAF 008, 018, 109) at room temperature. The band was detected by ImageQuant LAS4000 (GE healthcare). The same membrane was used for multiple western blot re-probing using stripping buffer (Thermo Sci. #21059). Western blots with  $\beta$ -actin antibody were performed as loading controls for cell lysates. Semi-quantitative measurements of band intensity were performed by densitometric analysis of immunoblots from different mice samples and shown as mean  $\pm$  SEM after normalization using loading controls. Bone marrow exudates were collected as previously described,<sup>4,5</sup> and used for immunoblot analyses. Western blots with total IgG antibody were performed as loading controls for BM exudates. A list of primary antibodies against specific proteins: VEGF (abcam, #ab46154, dilution: 1/1000), HIF-1 $\alpha$  (R&D, #AF1935, dilution: 1/400), VEGFR2 (Millipore, #07-716-1, dilution: 1/500), Tie2 (R&D, #AF762, dilution: 1/2000), P-p44/42 MAPK (Cell signaling, #9101, dilution: 1/1000), p44/42 MAPK (Cell signaling, #9102, dilution: 1/1000), angiopoietin-1 (Ang 1, abcam, dilution: 1/1000), angiopoietin 2 (Ang 2, abcam, clone EPR2891(2), dilution: 1/1000), and  $\beta$ -actin (Sigma, #2228, dilution: 1/2000), vascular cell adhesion molecule -1 (VCAM-1, R&D System, dilution: 1/1000), total IgG (Anti-mouse IgG-HRP, GE Healthcare Life Sciences, dilution 1/10,000), phospho (p)-Nrf2 (Phospho S40 Nrf2, abcam, clone EP1809Yb, dilution 1/1000), Nrf2 (abcam, dilution 1/1000), heme-oxygenase (HO-1, Santa Cruz Biotech, H-73, dilution

1/1000), endothelin-1 (ET-1, Santa Cruz Biotech, N-8, dilution 1/1000), and anti-GAPDH (Merck KGaA, dilution 1/5000).

**Soluble VCAM-1 measurements** The concentration of soluble VCAM-1 in mouse plasma was determined using the Mouse VCAM-1 ELISA Kit (CD106, Abcam), according to the manufacturer's instruction.

**Liver iron content (LIC)** Total non-heme iron content was determined using the bathophenanthroline method as previously described.<sup>12</sup> Briefly, about 100 mg of liver were dried at 110°C O/N, weight and digested in 1ml of 3 M HCl, 0.6 M Trichloroacetic acid for 20 hrs at 65°C. 5 µl of the supernatant were mixed in a chromogen solution (5 volumes of water, 5 volumes of saturated sodium acetate and 1 volume of 0.1% bathophenanthroline sulfonate/1% thioglycolic acid). The obtained colored product was measured spectrophotometrically at 535 nm and the concentration of non-heme iron was determined plotting onto a standard curve.<sup>13</sup>

**Immunofluorescence staining of cryopreserved sections of femurs** Whole mouse femurs were fixed in phosphate-buffered L-lysine with 1% paraformaldehyde /periodate (PLP), 16 h at 4°C, followed by washing in 0.1 M phosphate buffer pH 7.5, and cryoprotected for 72 h in 30% sucrose/0.1 M phosphate buffer. The fixed bones were embedded in OCT compound (optimal cutting temperature compound; a water-soluble glycol-resin compound; Sakura Finetek), snap frozen in 2-methylbutane/dry ice mix, and stored at -80°C. Fresh cryopreserved, non-decalcified femurs were sectioned longitudinally at 4- to 5-µm thickness to facilitate in situ laser scanning cytometry (LaSC) analysis of a single cell-thick layer using the CryoJane tape-transfer system (Instrumedics) in a cryostat (LEICA CM1800). All sections were prepared from the middle of the femur to include the central sinus. Thawed frozen sections were thoroughly air dried and rehydrated in D-PBS, followed by permeabilization in PBS-T (0.025% Tween 20 in Ca<sup>2+</sup>-free, Mg<sup>2+</sup>- free D-PBS) for 5 min. The sections were blocked in blocking medium (10% normal donkey serum/0.025% Tween 20 in Ca<sup>2+</sup>-free, Mg<sup>2+</sup>- free D-PBS) for 1 h, followed by streptavidin/biotin blocking solution (Vector

Laboratories). Bone sections were stained for 1h at room temperature or 16 h at 4°C with following specific primary antibodies: Sca-1 (D7; BioLegend, dilution 1/100), endoglin (AF1320; R&D, dilution 1/100), laminin (AB2034; Millipore, dilution 1/100), alpha smooth muscle actin ( $\alpha$ SMA; clone 1A4; Sigma-Aldrich, dilution 1/100), Ter119 (BioLegend, dilution 1/100), CD71 (Transferrin receptor; abcam #ab84036, dilution 1/200), Gr-1 (RB6-8C5; BioLegend, dilution 1/100), CD11b (M1/70; BioLegend, dilution 1/100), Ly6g (BioLegend, dilution 1/100), HIF-1 $\alpha$  (PA1-16601; Thermo Fisher, dilution 1/100), and GFP (chicken IgY; Invitrogen, dilution 1/200). After wash, the sections were stained with fluorescent dye (Dylight 488, Dylight 549, or Dylight 649)-labeled secondary antibodies against primary antibodies as follow: donkey anti-rat IgG, donkey anti-rabbit IgG, donkey anti-goat IgG, and donkey anti-chicken IgY (all secondary antibodies from Jackson ImmunoResearch, dilution 1/100). Dilutions of primary and secondary Abs were optimized for LaSC and confocal microscopy imaging. Isotype control slides were stained with Dylight 549–, Dylight 649–, or Dylight 488–labeled secondary Abs after isotype control primary Ab staining. All slides were then stained with 1  $\mu$ M DAPI for 3 min (Invitrogen), followed by mounting coverslips using SlowFade mounting media (Molecular Probes).

**In situ solid-phase LaSC analysis** For all LaSC analyses, the iCys Research Imaging Cytometer (CompuCyte) with four excitation lasers (405, 488, 561, and 633 nm), four emission filters (425–455, 500–550, 575–625, 650 nm long pass), and four photomultiplier tubes, was used. For each fluorescent marker, images are built pixel by pixel from the quantitative photomultiplier tube measurements of laser-spot excited fluorescence signals.<sup>14,15</sup> The quantitative imaging cytometry software iCys generated a single “region” image of the entire BM cavity from a sequence of high-magnification (40x/NA 0.95 dry objective) “field” immunofluorescence images (250  $\mu$ m x 190  $\mu$ m per field image) that were subjected to automated analysis of contour-based cellular events, their fluorescence levels, and their location within the BM section. Bone lining was identified by autofluorescence of the collagen in bone. Individual cellular events are defined by threshold contouring of DAPI-stained nuclei. In longitudinal BM sections, each femoral scan produces an average of 150,000 cellular events. The total

fluorescence intensity from individual cellular events is measured in each channel within the integration contour. The integration contour is set as two pixels out from the threshold contour, a value that is based on the size of the cell, to allow definition of the edge of the cell (pixel size is 0.25  $\mu\text{m}$  x 0.25  $\mu\text{m}$ ). Specific types of cellular events and niche components were systemically identified by image segmentation on specific fluorescent signals with iCys analysis software as follows: arterioles/arteries by Sca-1<sup>+</sup> events, neo-vascularized arteriolar/arterial pericytes by  $\alpha\text{SMA}^+$  events, sinusoids by endoglin<sup>+</sup> events, apoptotic cells by TUNEL<sup>+</sup> events, hypoxia-induced signaling cells by DAPI<sup>+</sup> HIF-1 $\alpha^{\text{hi}}$  cells, CAR cell by DAPI<sup>+</sup> CXCL12-GFP<sup>hi</sup> events. Individual cellular and niche events were systematically visualized and confirmed by morphology. Isotype antibodies were used as negative controls for gating purposes. The total number and morphological distribution of each distinct cellular subpopulation within the entire femoral BM cavity or at specific anatomical locations within the cavity can then be determined using post-scan automated image analysis software (iCys cytometric analysis software; CompuCyte). To assess statistical significance, we analyzed 3 distinct frozen longitudinal sections per femur from 4 mice each, total 12 sections.

**H & E staining of cryopreserved sections of femurs for Histopathology** After LaSC imaging acquisition, slides with PLP-fixed thin sections were washed with D-PBS followed by H&E (hematoxylin-eosin) staining by standard methods for the analysis of histopathological conditions of SCD mouse BM. Photomicrographs were made using light microscope Olympus BX51 with Spot software 5.1 (Diagnostic Instruments) and formatted using Adobe Photoshop (Adobe Systems).

**Whole-mount immunostaining of femoral BM slices for confocal microscopy** PLP-fixed femurs were embedded in OCT block and frozen as described above. OCT-embedded frozen femurs were trimmed by a cryostat to expose fully BM cavity along the longitudinal axis, followed by repeating same process on the other side of bone until a thick BM slice was obtained. After removing OCT medium in PBS, BM slices were blocked overnight at 4°C in blocking solution (0.2% Triton X-100, 1% BSA, and 10% donkey serum in PBS with sodium azide). BM slices were stained with goat anti-

endoglin and rat anti-Sca-1 antibodies for 3 days in blocking solution at 4°C, washed 3 times 30 min each in PBS, and stained with secondary antibodies overnight at 4°C. Whole-mount stained slices were then washed in PBS and stained with 1 μM DAPI for 20 min, followed by overnight incubation in FocusClear (CelExplorer Lab) with 1 μM DAPI at 4°C. BM slices were embedded in FocusClear and mounted on glass slides for observation under the confocal microscope (Leica SP8X, Neurobiology Imaging Facility at Harvard Medical School).

**Confocal microscopy and image processing** Leica SP8X confocal microscopy (HC PL APO 10x/NA 0.40 dry CS or HC PL APO 40x/NA 1.3 oil CS2 objectives) was equipped with the White Light Laser (continuous excitation tuning from 470 nm to 670 nm), 405 nm DPSS laser, 4 detectors (two HyD and two PMT) controlled by Microscope Imaging Software LAS X (Leica Microsystems). Z-stacks of images were processed and 3D-reconstructed with Volocity software (PerkinElmer). Volocity software generated 3D movie files showing a 360° horizontal rotation of the stacks. 3D volumetric quantifications of segmented BM components were done with Volocity software on high resolution confocal images. Sca-1<sup>+</sup> volumes were calculated by multiplying the total number of Sca-1<sup>+</sup> objects by the mean voxel volume. BM volume in 3D reconstructed images was calculated from segmented DAPI<sup>+</sup> objects by applying sequential filters, i.e. threshold-opening-closing-fill holes.<sup>16</sup> % BM volume of Sca-1<sup>+</sup> arterioles/arteries = Sca-1<sup>+</sup> volumes/ BM volume x 100.

**Blood cell velocity quantification in bone marrow vasculature** To visualize skull bone marrow vasculature and to identify RBCs inside vessels by negative contrast, 40 μl of cell-impermeable rhodamine B-dextran 70 kDa (10 mg/ml) was injected to mice retro-orbitally. Videos of images of blood vessel (Rhodamine B, excitation: 561 nm, emission: 573–613 nm) were taken with the speed of 120 frames per second by using confocal intravital microscope. In the vascular image, blood plasma mixed with the rhodamine B-dextran was shown as bright contrast while endogenous blood cells were shown as dark contrast. In each vessel segment with 5 s x 120 frames/sec, blood cell flow speed was measured from a representative RBC out of more than 20 RBCs as



shown in a schematic illustration (see Supplemental Figure S2A). For the exogenous wild type blood cell speed measurement, C57BL/6 wild type red blood cells (RBCs) were labelled with 15  $\mu$ M CFSE (Invitrogen) for 12 min at 37 °C in PBS supplemented with 1 g per litre of glucose and 0.1% BSA. About 0.6 billion RBCs were injected (i.v.) with 40  $\mu$ l of rhodamine B-dextran 70 kDa (10 mg/ml) retro-orbitally immediately before imaging. Total displacement of the blood cells was measured by ImageJ and the speed of blood cells was calculated by:

Total displacement of blood cells ( $\mu$ m) / Time (=number of frames x 1/120 sec)

The total displacement can be accurately measured by performing repetitive laser line scanning along the long axis of the blood vessel and acquiring space-time image as reported in the previous research.<sup>17,18</sup> In our flow speed measurement, instead of physical laser line scanning, digital line scanning on the recorded video was performed, and blood flow speed from multiple blood vessel segments in the field of view was acquired.

**Statistical analysis** All data are presented as mean  $\pm$  SEM (standard error of mean). All statistical analysis was performed using Prism 8 software (GraphPad). The significance of difference in the mean values of two conditions was determined using two-tailed Student's t-test unless indicated otherwise. Flow speeds of blood cells were analyzed with a linear mixed model analysis using SAS (version 9.4). For experiments that involved multiple comparison t-tests, a Bonferroni adjustment was applied as indicated. Comparisons of other multiple treatments were made by ANOVA with Tukey test or Dunnet's test as indicated. P value less than 0.05 ( $p < 0.05$ ) was considered significant. For graphs representing LaSC data, single femurs from different mice analyzed were considered as independent data points ( $n$  = number of mice). When multiple sections from a single femur were analyzed, the results were treated as technical replicates that were averaged and considered as one single independent sample for statistical purposes. The numbers of independent mouse samples in each experiment are provided in the figure legends. Sample sizes were selected by power analysis using PASS software (Version 15.0, NCSS) as previously described. Statistical significance and P values are indicated by asterisks and specified in the figure legends.

## REFERENCES

1. Ara T, Tokoyoda K, Sugiyama T, Egawa T, Kawabata K, Nagasawa T. Long-term hematopoietic stem cells require stromal cell-derived factor-1 for colonizing bone marrow during ontogeny. *Immunity*. 2003;19(2):257-267.
2. Sugiyama T, Kohara H, Noda M, Nagasawa T. Maintenance of the hematopoietic stem cell pool by CXCL12-CXCR4 chemokine signaling in bone marrow stromal cell niches. *Immunity*. 2006;25(6):977-988.
3. Dalle Carbonare L, Matte A, Valenti MT, et al. Hypoxia-reperfusion affects osteogenic lineage and promotes sickle cell bone disease. *Blood*. 2015;126(20):2320-2328.
4. Eash KJ, Greenbaum AM, Gopalan PK, Link DC. CXCR2 and CXCR4 antagonistically regulate neutrophil trafficking from murine bone marrow. *J Clin Invest*. 2010;120(7):2423-2431.
5. Fan Y, Hanai JI, Le PT, et al. Parathyroid Hormone Directs Bone Marrow Mesenchymal Cell Fate. *Cell Metab*. 2017;25(3):661-672.
6. La Carpia F WB, Rebbaa A, Tang A, Hod EA. Chronic transfusion and iron overload modify the mouse gut microbiome. In: BLOOD ed. ASH. Atlanta: Blood; 2016:200.
7. Kalish BT, Matte A, Andolfo I, et al. Dietary omega-3 fatty acids protect against vasculopathy in a transgenic mouse model of sickle cell disease. *Haematologica*. 2015;100(7):870-880.
8. Matte A, Recchiuti A, Federti E, et al. Resolution of sickle cell disease-associated inflammation and tissue damage with 17R-resolvin D1. *Blood*. 2019;133(3):252-265.
9. Matte A, De Falco L, Federti E, et al. Peroxiredoxin-2: A Novel Regulator of Iron Homeostasis in Ineffective Erythropoiesis. *Antioxid Redox Signal*. 2018;28(1):1-14.
10. Matte A, De Falco L, Iolascon A, et al. The Interplay Between Peroxiredoxin-2 and Nuclear Factor-Erythroid 2 Is Important in Limiting Oxidative Mediated Dysfunction in beta-Thalassemic Erythropoiesis. *Antioxid Redox Signal*. 2015;23(16):1284-1297.
11. Houlihan DD, Mabuchi Y, Morikawa S, et al. Isolation of mouse mesenchymal stem cells on the basis of expression of Sca-1 and PDGFR-alpha. *Nat Protoc*. 2012;7(12):2103-2111.
12. Bellelli R, Federico G, Matte A, et al. NCOA4 Deficiency Impairs Systemic Iron Homeostasis. *Cell Rep*. 2016;14(3):411-421.
13. Nai A, Pagani A, Mandelli G, et al. Deletion of Tmprss6 attenuates the phenotype in a mouse model of beta-thalassemia. *Blood*. 2012;119(21):5021-5029.
14. Nombela-Arrieta C, Pivarnik G, Winkel B, et al. Quantitative imaging of haematopoietic stem and progenitor cell localization and hypoxic status in the bone marrow microenvironment. *Nat Cell Biol*. 2013;15(5):533-543.
15. Park SY, Wolfram P, Canty K, et al. Focal adhesion kinase regulates the localization and retention of pro-B cells in bone marrow microenvironments. *J Immunol*. 2013;190(3):1094-1102.
16. Gomariz A, Helbling PM, Isringhausen S, et al. Quantitative spatial analysis of haematopoiesis-regulating stromal cells in the bone marrow microenvironment by 3D microscopy. *Nat Commun*. 2018;9(1):2532.

17. Drew PJ, Blinder P, Cauwenberghs G, Shih AY, Kleinfeld D. Rapid determination of particle velocity from space-time images using the Radon transform. *J Comput Neurosci*. 2010;29(1-2):5-11.
18. Shih AY, Driscoll JD, Drew PJ, Nishimura N, Schaffer CB, Kleinfeld D. Two-photon microscopy as a tool to study blood flow and neurovascular coupling in the rodent brain. *J Cereb Blood Flow Metab*. 2012;32(7):1277-1309.
19. Colvin GA, Lambert JF, Abedi M, et al. Murine marrow cellularity and the concept of stem cell competition: geographic and quantitative determinants in stem cell biology. *Leukemia*. 2004;18(3):575-583.

## Supplemental Figure legends

### Supplemental Figure S1. Analysis of SCD BM by LaSC and histopathology. (A)

LaSC analysis of Sca-1<sup>+</sup> BM area analysis in the BM. Longitudinal thin frozen sections of femurs (5 μm thickness) of 12 week old AA and SS mice were stained with rat antibodies against Sca-1, followed by secondary antibodies (Alexa 488- conjugated donkey anti-rat). After nuclear DAPI staining, whole femoral sections were scanned for high- resolution field images by LaSC. From 2D laser scanning cytometry images of 3 sections each per mouse, quantification of Sca-1<sup>+</sup> BM area was performed by iCys software (CompuCyte). Arteries/arterioles were identified by Sca-1<sup>+</sup> contours in the diaphysis. BM cell events were identified by DAPI<sup>+</sup> contours. Distribution of DAPI<sup>+</sup> or Sca-1<sup>+</sup> contoured events was plotted in scattergrams with xy-position. Mean area of Sca-1<sup>+</sup> events was calculated by iCys software. Sca-1<sup>+</sup> BM area (μm<sup>2</sup>) per 100K BM cells = (Sca-1<sup>+</sup> event #) x (mean area of Sca-1<sup>+</sup> events) / (DAPI<sup>+</sup> cell #) x 100,000. Quantitation of Sca-1<sup>+</sup> BM area was done with iCys LaSC software and is shown in Figure 1C. (B) Histopathology in SCD mouse BM. After LaSC imaging acquisition, slides with thin frozen sections were washed with D-PBS followed by H&E staining for the analysis of histopathological conditions of SCD mouse BM (60x/NA1.4 oil objective). Representative images of femoral sections are shown from 9-16 week old 4 AA and 4 SS mice. An arrow indicates congested vascular area with RBC aggregates.

### Supplemental Figure S2. RBC flow speed measurement in SCD mouse BM vasculature.

(A) Schematic illustration of RBC flow speed measurement by negative contrast. B. The flow speed of CFSE-labeled wild type RBCs is slow in SCD mice compared to control mice. (B and C) 600 millions of CFSE-labeled RBCs from WT mice were injected into SCD SS mice or control (AA or WT) mice. After retro-orbital injection CFSE-labeled RBC with rhodamine B-dextran 70 kDa, blood cells flowing in calvarial BM vasculature were recorded using confocal IVM, followed by calculation of blood cell flow speed (displacement over time) using ImageJ as described in Supplemental Methods. (B) Values of flow speed per cell were plotted as scatter dot plots for each individual mouse with a mean of individual mouse and pooled total shown as narrower and broader horizontal lines, respectively, by Prism 8 software (GraphPad). Each dot

represents individual CFSE-labeled RBC. Numbers of cells plotted per mouse (total 4 mice) were 27, 13, 9, 7 (AA)/ 29, 14, 8, 3 (SS) for arterioles and 16, 9, 5, 7 (AA)/ 14, 11, 11, 6 (SS) for sinusoids, respectively. Indicated p values were analyzed by generalized linear model (GLM) with a random effect of mouse nested within genotype (n=4 mice). (C) The mean flow speed of CFSE-labeled wild type RBCs per mouse were plotted as bar graphs with mean  $\pm$  SEM. The mean CFSE-labeled RBC flow speeds of each mouse were represented as dots. Student's t-test, \*\*p <0.01, n = 4 mice (12-15 week old 2 female and 2 male mice).

**Supplemental Figure S3. Analysis of hypoxia-induced signaling molecules in SCD peripheral plasma.** (A) Left panel. Immuno-blot analysis with specific antibodies against vascular endothelial growth factor-A (VEGF-A), angiopoietin-1 (Ang 1), angiopoietin 2 (Ang 2), vascular cell adhesion molecule-1 (VCAM-1) of peripheral plasma from AA and SS mice. Total IgG was used as a loading control. One representative gel out of 6 with similar results is presented. Right panel. Data from densitometric analysis of the immunoblots are shown as protein intensity relative to IgG. Results are presented as mean  $\pm$  SEM (n=6 from each strain, 12-15 week old 3 female and 3 male mice in each group were analyzed) (AU: arbitrary units). Ang 2 represents both immature and mature Ang 2 forms. (B) Soluble Vascular Cell Adhesion Molecule-1 (sVCAM1) concentration in plasma from healthy (AA) and sickle cell (SS) mice was measured by ELISA. Data are shown as mean  $\pm$ SEM (n=6 from 12-15 week old 3 female and 3 male mice in each group were analyzed; Student's t-test, \* p<0.05 compared to AA).

**Supplemental Figure S4. Analysis of expanded erythropoietic activity in the BM and extramedullary splenic erythropoiesis by CD71-Ter119 gating strategy.** (A) Cyto-fluorimetric analysis of total erythroid precursors from the bone marrow and the spleen of AA and SS mice was done using CD71-Ter119 in bone marrow and spleen. (B) Erythroblast subpopulations determined by CD71-Ter119 gating strategy. Population I (Pop I) corresponds to pro-erythroblasts, population II (Pop II), corresponds to basophilic erythroblasts; population III (Pop III), corresponds to polychromatic

erythroblasts and population IV (Pop IV), corresponds to orthochromatic erythroblasts. All graphs were presented as mean  $\pm$ SEM, n=6 (14-16 week old 4 female and 2 male mice in each group). Student's t-test, \*p<0.05 compared to healthy AA mice.

**Supplemental Figure S5. LaSC analysis strategy of perisinusoidal or non-perisinusoidal CXCL12-GFP<sup>hi</sup> CAR cells in the CXCL12-GFP<sup>+</sup> BM.** Femoral frozen sections (5  $\mu$ m thickness) of 12 week old CXCL12-GFP<sup>+</sup> mice were stained with chicken antibodies against GFP and goat antibodies against endoglin, followed by secondary antibodies (Alexa 488- conjugated donkey anti-chicken and Alexa 546- conjugated donkey anti-goat, respectively). After nuclear DAPI staining, whole femoral sections were scanned for high- resolution field images by LaSC. Sinusoids were identified by Endoglin<sup>+</sup> contours (see right side upper panels). CAR cell events were identified by DAPI<sup>+</sup> CXCL12-GFP<sup>hi</sup> events (see right side middle panels). CAR cell events within 5  $\mu$ m periphery of Endoglin<sup>+</sup> contour were defined as perisinusoidal events (e.g. a CAR cell pointed by an arrowhead), while other CAR cell events were defined as non-perisinusoidal events (e.g. a CAR cell pointed by an arrow). Quantitation of CAR cell numbers in perisinusoidal area and non-perisinusoidal area was done with iCys LaSC software and is shown in Figure 5.

**Supplemental Figure S6. The abnormal vascular niche impacts steady-state hematopoiesis.** (A) HSPCs were analyzed in the spleen of SS and AA mice by Attune NxT flow cytometer (Thermo Fisher) using specific antibodies: CD48-FITC, CD34-eF660, CD135-BV421, Sca-1-BV711, CD150-PE, c-Kit-PE-Dazzle594, CD16/32-PE-Cy7, and biotinylated lineage markers (B220, CD19, CD11b, Gr-1, CD3e, CD4, CD8, Ter119, and CD5) followed by streptavidin-BV605. The frequencies in each gate indicate the percentage of total MNCs. Cellularity of bone marrow and spleen was calculated using flow cytometry analysis. (B) Total BM cellularity was calculated from 2 limbs that contain 14% of all BM cells<sup>19</sup> and plotted, n=5 (9-16 week old 2 female and 3 male mice). (C) The numbers of HSPCs are increased in the BM and the spleen of SS mice. BM and spleen cells were prepared from SCD SS and control AA mice and stained with specific antibodies for HSPC subpopulations, followed by flow cytometry.

Absolute numbers of HSPC subpopulations in total BM, and spleen were calculated based on the gating strategy shown in the Supplemental Figure S6A. Graphs were plotted for subpopulations of LSK cells (Lineage<sup>-</sup> Sca-1<sup>+</sup> c-Kit<sup>+</sup>; upper panel) including LT-HSCs (CD34<sup>-</sup> CD135<sup>-</sup> CD48<sup>-</sup> CD150<sup>+</sup> LSKs), MPP1 (CD34<sup>+</sup> CD135<sup>-</sup> CD48<sup>-</sup> CD150<sup>+</sup> LSKs), MPP2 (CD34<sup>+</sup> CD135<sup>-</sup> CD48<sup>+</sup> CD150<sup>+</sup> LSKs), MPP3 (CD34<sup>+</sup> CD135<sup>-</sup> CD48<sup>+</sup> CD150<sup>-</sup> LSKs), MPP4 (CD34<sup>+</sup> CD135<sup>+</sup> CD48<sup>+</sup> CD150<sup>-</sup> LSKs); and for subpopulations of LK cells (Lineage<sup>-</sup> Sca-1<sup>-</sup> c-Kit<sup>+</sup>; lower panel) including CMP (CD34<sup>+</sup> CD16/32<sup>lo</sup> LKs), GMP (CD34<sup>+</sup> CD16/32<sup>hi</sup> LKs), MEP (CD34<sup>-</sup> CD16/32<sup>-</sup> LKs), n=5 (9-16 week old 2 female and 3 male mice). (D) Increased circulating colony forming HSPCs and mature leukocytes in the peripheral blood of SCD mice. Colony forming HSPCs were analyzed by MethoCult-based CFU-C (colony forming units in culture) assay kit (Stem Cell Technologies) from the PB of AA and SS mice according to manufacturer's instruction. Colony numbers were counted on 7-10 days after plating. The classes of colonies (CFU-GEMM, CFU-G, CFU-M, CFU-GM, and BFU-E) were identified by the morphology of colonies according to manufacturer's instruction. The # of CFU-C in 3 groups (CFU-GEMM, CFU-G/M/GM, and BFU-E) were plotted, n=4 (9-12 week old 2 female and 2 male mice). (E) Flow cytometry analysis was performed to quantitate myeloid (Gr-1) and lymphoid (B220<sup>+</sup> B cells or CD3e<sup>+</sup> T cells) mononuclear cell numbers in the PB of AA and SS mice, n=6 (9-16 week old 3 female and 3 male mice). All bar graphs were plotted as mean ± SEM, two-tailed unpaired student's t-test \*p<0.05, \*\*p<0.01, \*\*\*p<0.001.

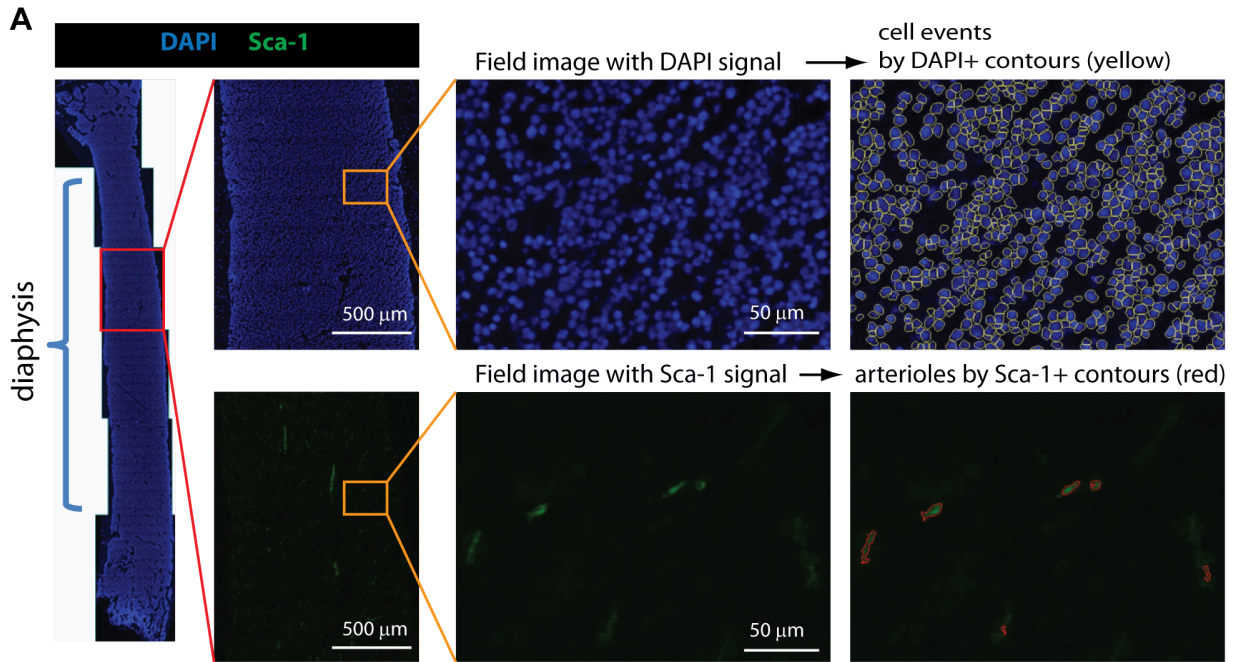
**Supplemental Figure S7. Splenomegaly and BM vascular niche defects are reversed by 6-week blood cell transfusion regimen.** (A) Spleen volume as determined by in vivo abdominal Ultrasound analysis in AA and SS mice treated with either vehicle or red blood cell (RBC) transfusion at 3 and 6 weeks of treatment. Data are shown as median values, n=3 (12-15 week old 1 female and 2 male mice), two-way ANOVA with Bonferroni correction for multiple comparisons. (B) ROS levels in erythroid precursors from the bone marrow of AA and SS mice treated with either vehicle or RBC transfusion for 6 weeks. Data are presented as mean ±SEM, n=6 (12-15 week old 3 female and 3 male mice), two-way ANOVA with Bonferroni correction for

multiple comparisons. (C) Left panel. Immuno-blot analysis with specific antibodies against VEGF-A, Ang 1, Ang 2, and VCAM-1 of peripheral plasma from SS mice treated with either vehicle or RBC transfusion for 6 weeks. Right panel. Data from densitometric analysis are presented as mean  $\pm$  SEM (n=6 from each strain, 12-15 week old 3 female and 3 male mice in each group were analyzed) (AU: arbitrary units); two-way ANOVA with Bonferroni correction for multiple comparisons. Ang 2 represents both immature and mature forms. (D) Soluble Vascular Cell Adhesion Molecule-1 (sVCAM1) concentration in plasma from SS mice treated with either vehicle or RBC transfusion at 3 and 6 weeks of therapy was measured by ELISA. Data are presented as mean  $\pm$  SEM (n=6 from each strain, 12-15 week old 3 female and 3 male mice in each group were analyzed). (E) Left panel. Immuno-blot analysis with specific antibodies against phospho(p)-Nrf2 and total Nrf2, as well as against heme-oxygenase (HO-1) and endothelin-1 (ET-1) of lung from AA and SS mice treated with either vehicle or transfusion (6 weeks). Right panel. Data from densitometric analysis are presented as mean  $\pm$  SEM (n=6 from each strain, 12-15 week old 3 female and 3 male mice in each group were analyzed). Two-way ANOVA with Bonferroni correction for multiple comparisons. (F and G) Left panel. Immuno-blot analysis with specific antibodies against heme-oxygenase (HO-1) of liver (F) and heart (G) from AA and SS mice treated with either vehicle or transfusion (3 or 6 weeks). Right panel. Data from densitometric analysis are presented as mean  $\pm$  SEM (n=6 from each strain, 12-15 weeks old 3 female and 3 male mice in each group were analyzed). Two-way ANOVA with Bonferroni correction for multiple comparisons. H. Liver iron content (LIC) in AA and SS mice treated with either vehicle or transfusion (6 weeks). Results are presented as mean  $\pm$  SEM (n=4 from each strain, 12-15 weeks old 3 female and 3 male mice in each group were analyzed). Two-way ANOVA with Bonferroni correction for multiple comparisons. P values: \*p<0.05 compared to healthy AA mice, °p<0.05 compared to vehicle treated SS animals. For immunoblots (C, E, F, and G) with one representative gel from 6 mice with similar results, data from densitometric analysis of the immunoblots are shown as protein intensity relative to loading controls, i.e. IgG light chain (LC) or GAPDH. AU= arbitrary units.

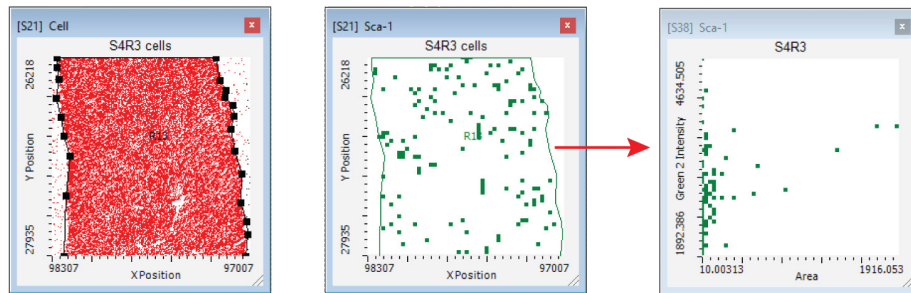


**Supplemental Figure S8. The reversal of BM vascular niche defects by 6-week blood cell transfusion regimen were confirmed by histopathology and LaSC imaging of Ter119<sup>+</sup> RBC aggregates in the femoral BM.** (A) Histopathology was reversed by 6-week blood cell transfusion in SCD mouse BM. After LaSC imaging acquisition, slides with thin sections were washed with D-PBS followed by H&E staining for the analysis of histopathological conditions of SCD mouse BM (40x/NA 0.5 objective). In SS mice, an arrow indicates congested vascular area with RBC aggregates that were not found in 6-week blood transfused SS mice. Representative images of femoral sections are shown from 12-15 week old three mice. (B) Ter119<sup>+</sup> RBC aggregates in the femoral BM sections of AA, SS+vehicle, and SS+RBC transfusion mice were analyzed by LaSC. Arrows indicate sRBC aggregates in Endoglin (Edgn)<sup>+</sup> sinusoids. Representative images of femoral sections are shown from 12-15 week old three mice.

# Supplemental Figure S1



↓ Distribution of contoured events in scattergrams



DAPI+ cell event numbers = 33,563

Sca-1+ arteriole event numbers = 153

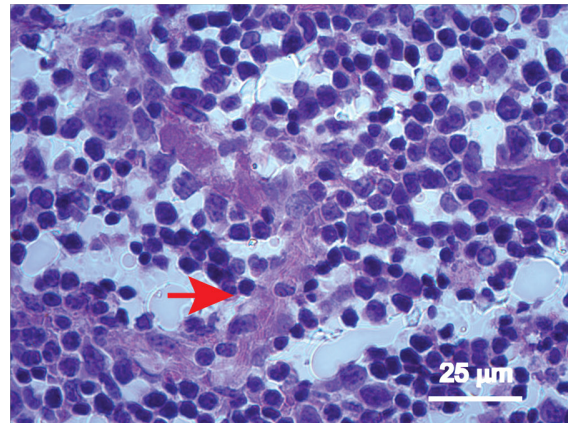
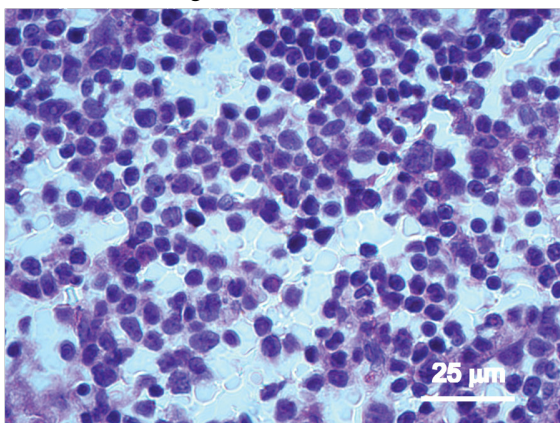
Mean area of Sca-1+ events = 91.2 μm<sup>2</sup>

$$* \text{ Sca-1+ BM area per 100K cells} = \frac{(\text{Sca-1+ event \#}) \times (\text{mean area of Sca-1+ events})}{(\text{DAPI+ cell \#}) \times 100,000}$$

**B** BM H&E staining:

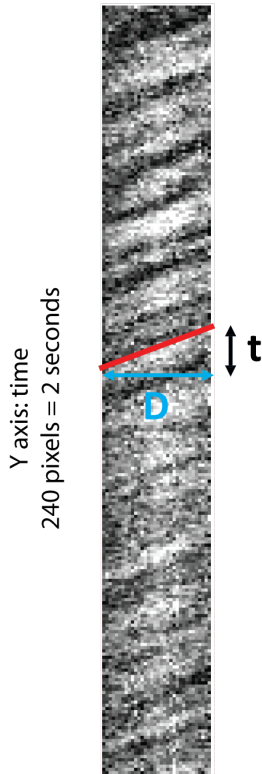
AA

SS



## Supplemental Figure S2

**A** X axis: distance  
34 pixels (0.73  $\mu\text{m}/\text{pixel}$ )



Measurement of the blood cell flow speed by negative contrast

1. A distance (X-axis) vs. time (Y-axis) image from an intravital microscopy video shows a pattern of dark lines by negative contrast.

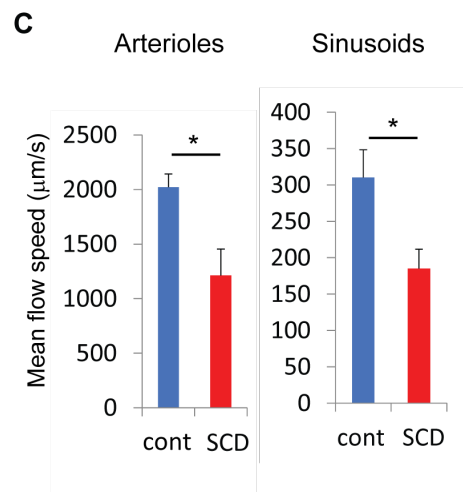
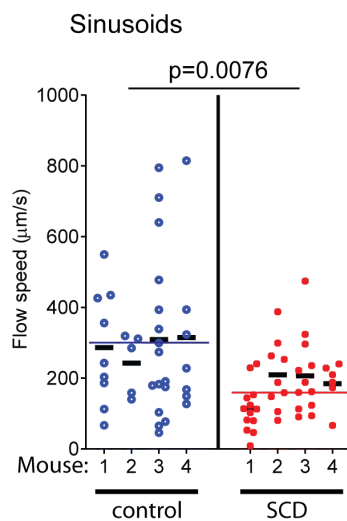
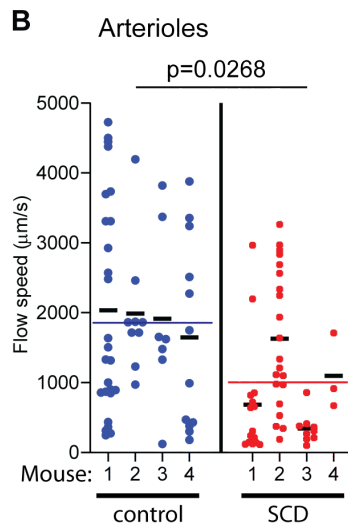
2. Each (slanted) dark line represents the trace of an RBC. The slope of dark lines indicate flow speed. In this figure there are about 18 dark lines, representing 18 RBCs with an essentially same slope, meaning that all the RBCs in this vessel segment are traveling at about the same speed.

3. Blood cell flow speed is measured from a representative dark contrast line (solid red line) in the vessel segment.

Time (t): 15 pixels =  $1/120 \times 15 = 0.125$  seconds

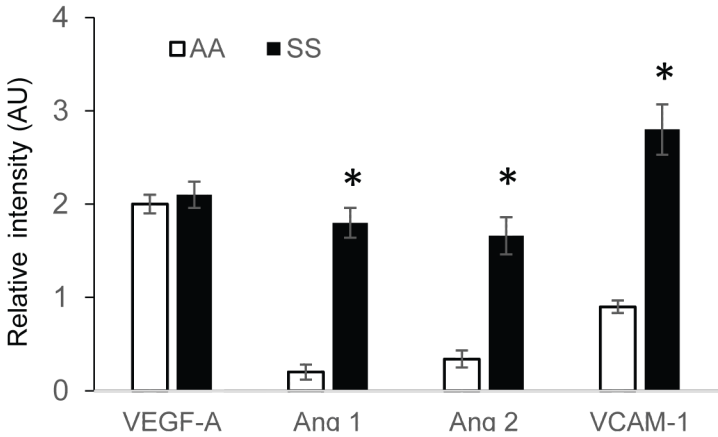
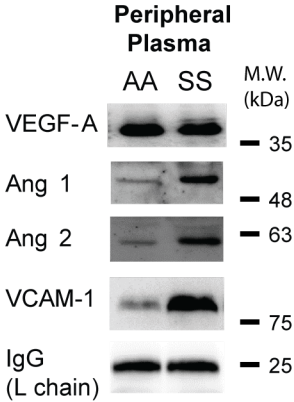
Distance (D): 34 pixels =  $34 \times 0.73 \mu\text{m} = 24.82 \mu\text{m}$

Speed = distance (D) / time (t) =  $24.82 / 0.125 = 199 \mu\text{m}/\text{s}$

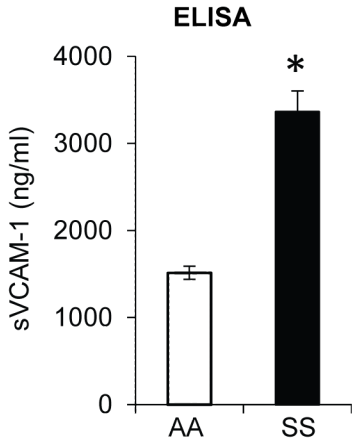


**Supplemental Figure S3**

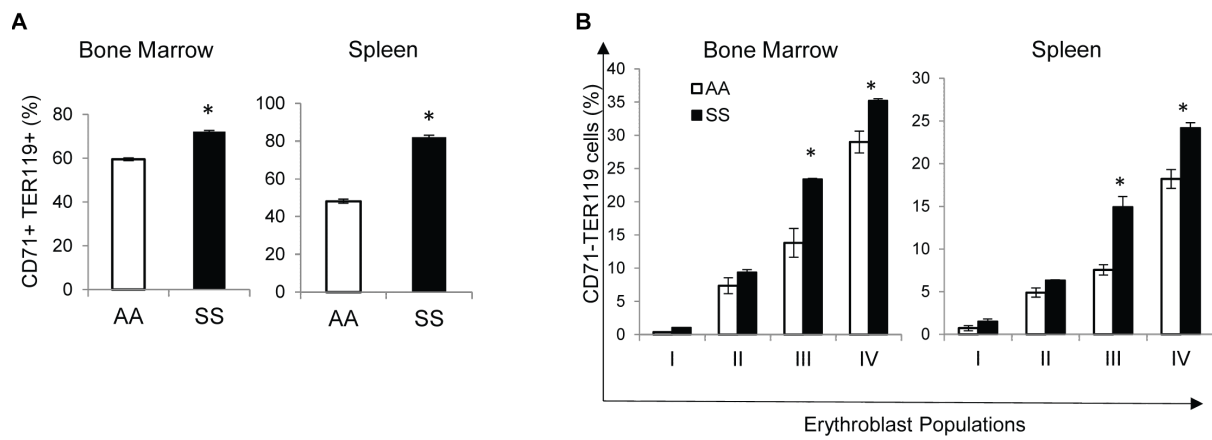
**A**



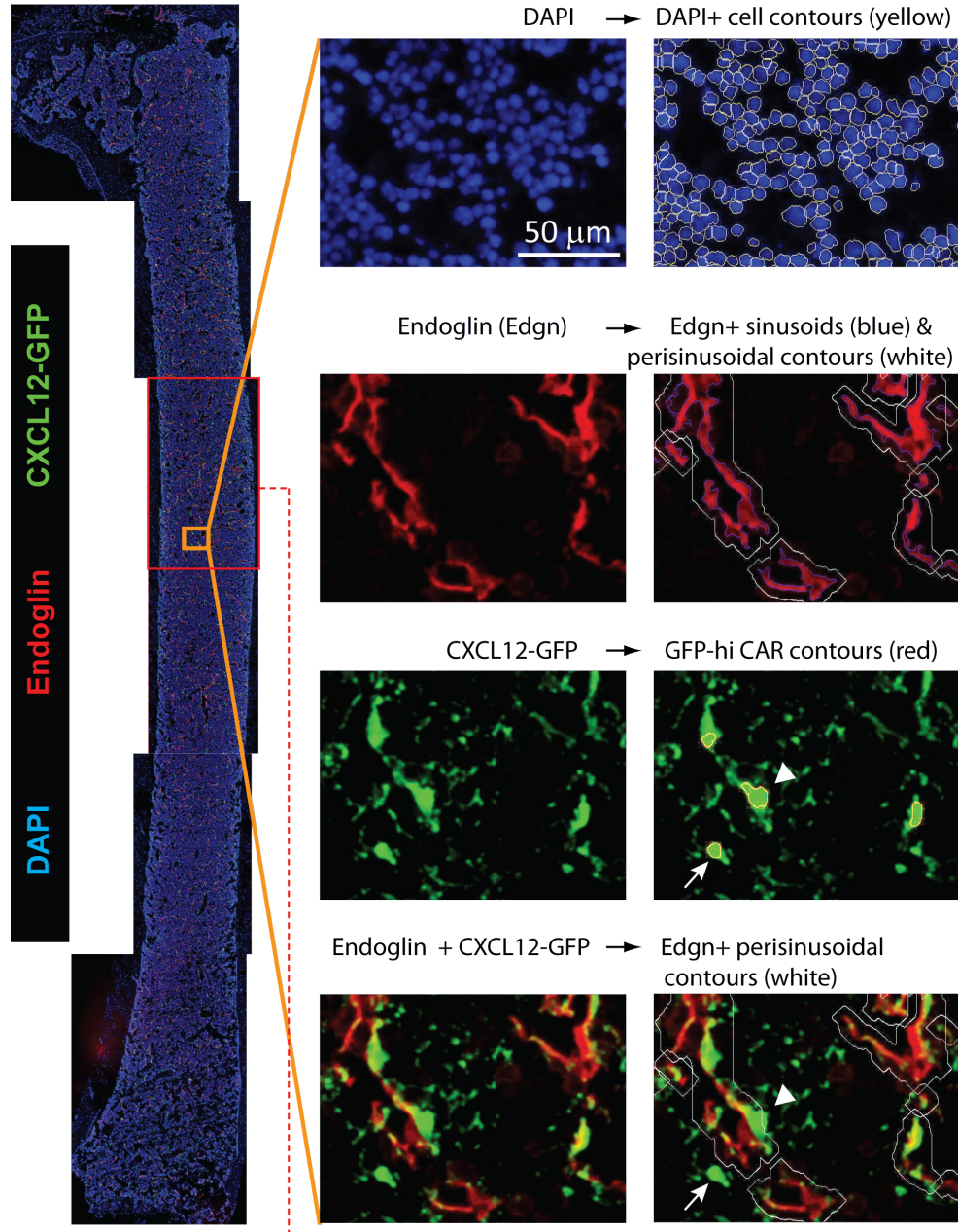
**B**



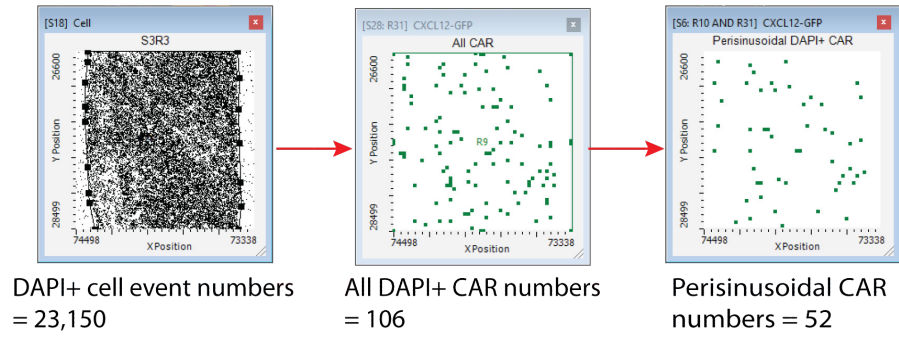
## Supplemental Figure S4



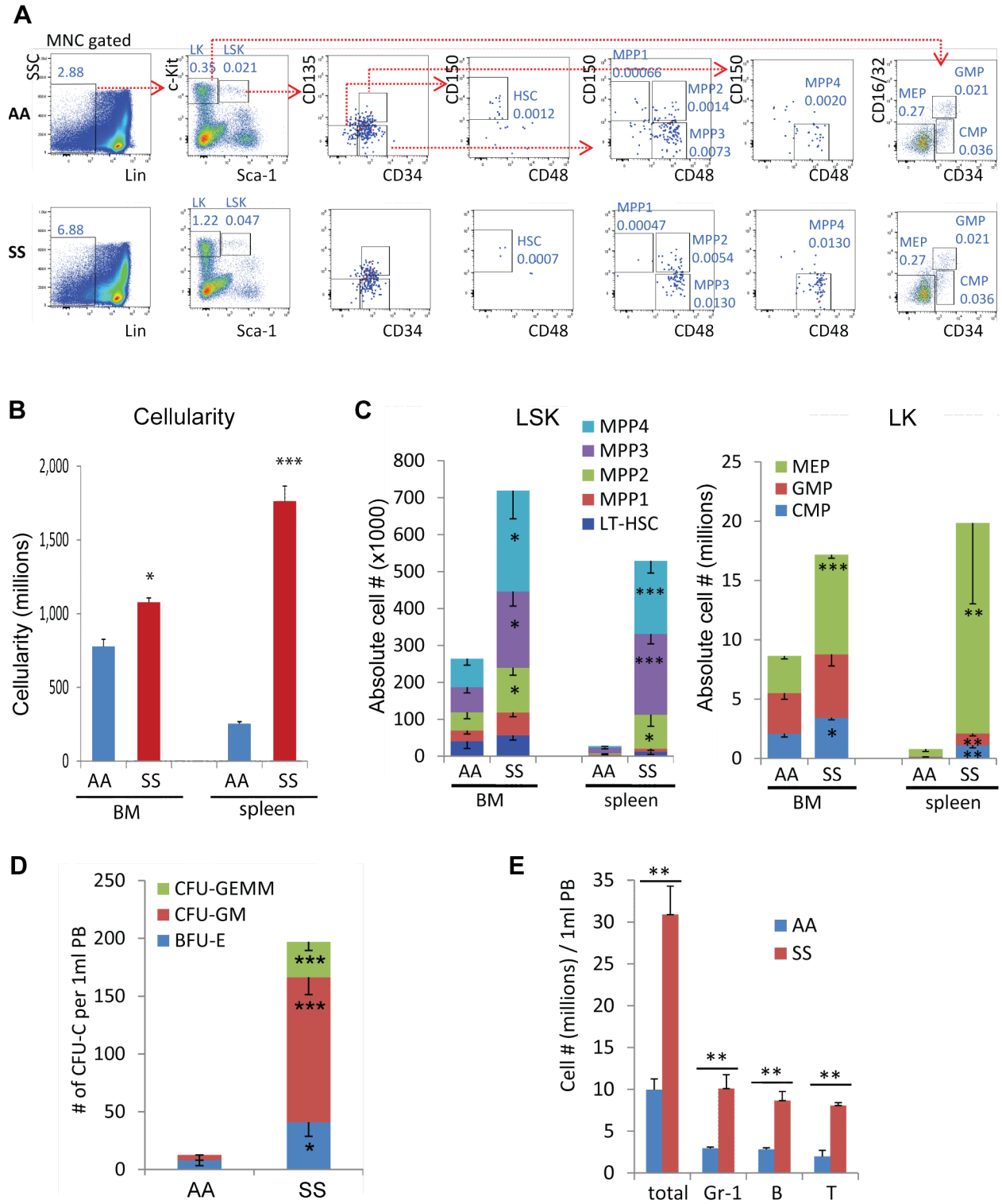
# Supplemental Figure S5



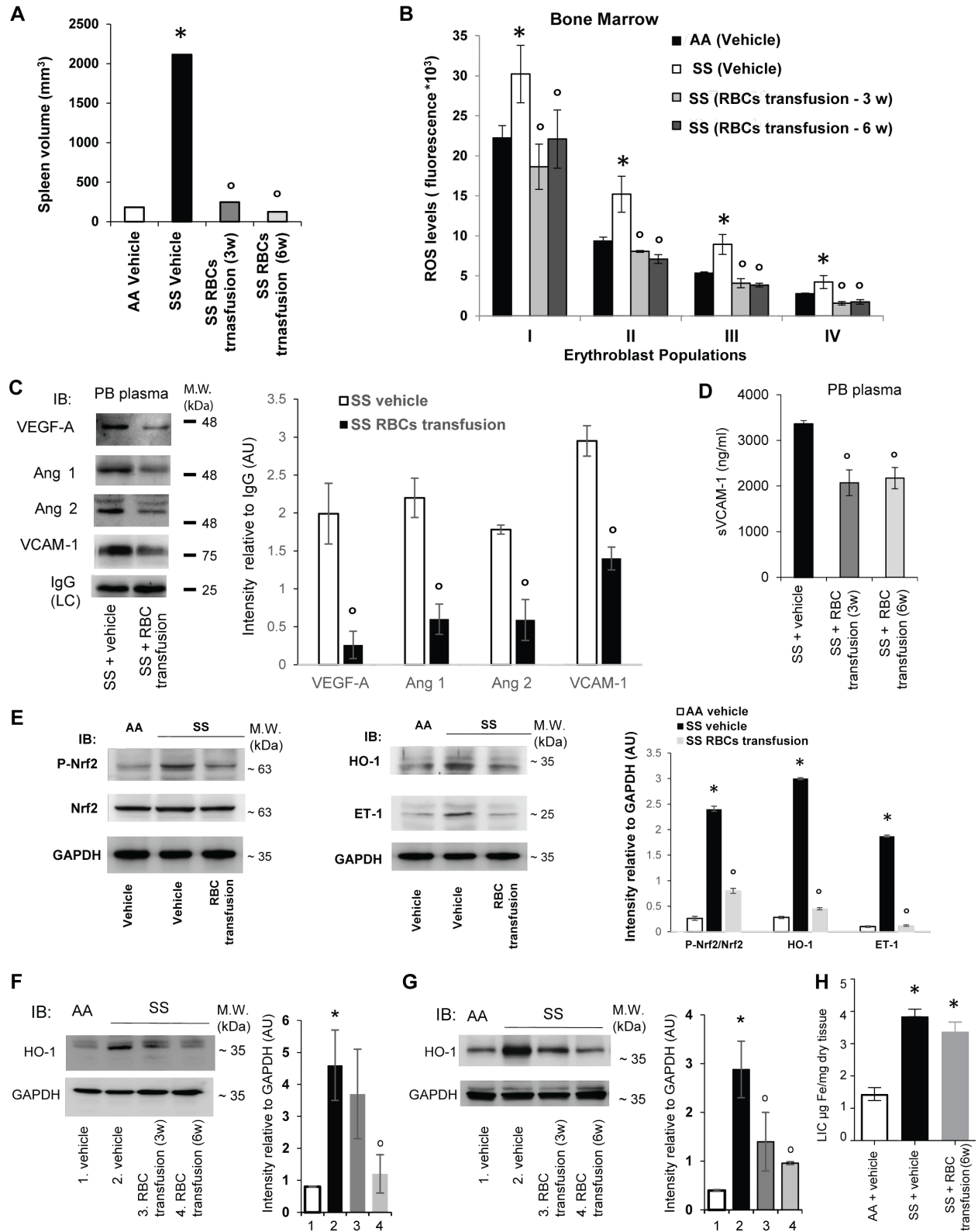
↓ Distribution of contoured events in scattergrams



## Supplemental Figure S6



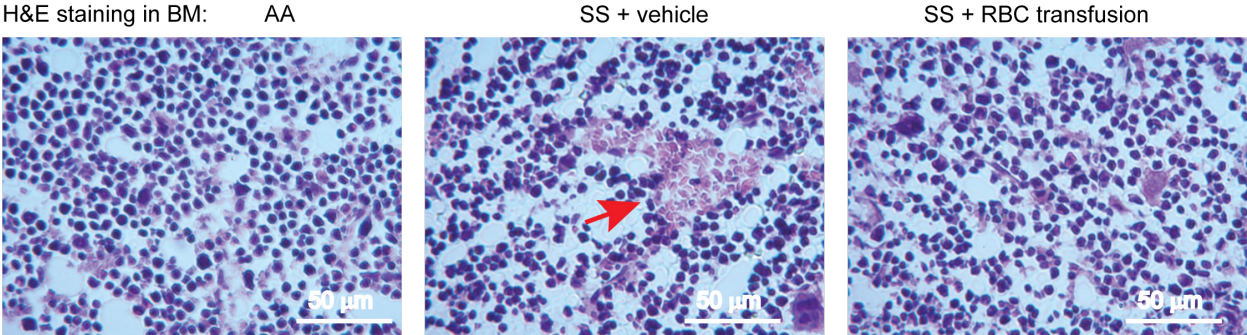
# Supplemental Figure S7



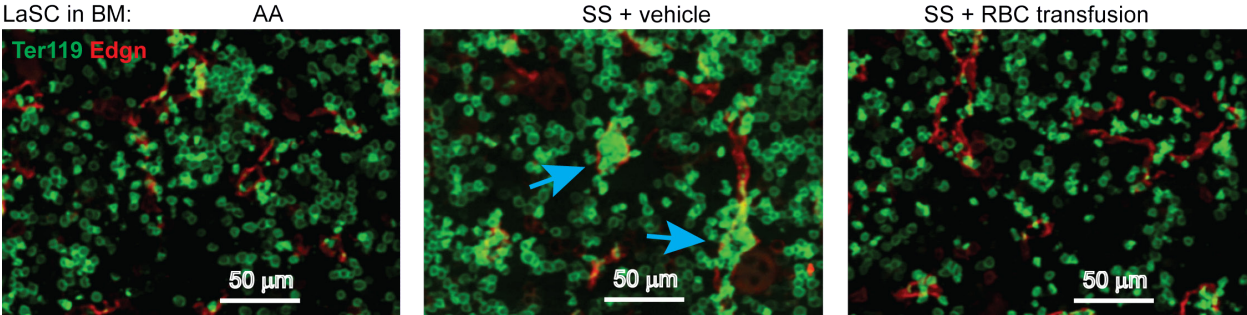


# Supplemental Figure S8

A



B



## Legends for Videos

**Supplemental Video 1.** Normal BM vasculature in control mouse. 3D-reconstruction of confocal optical sections (LEICA SP8X, 10x objective) of thick femoral slices stained for pan-vasculature marker laminin (green), sinusoid marker endoglin (red), and arteriole/artery marker Sca-1 (blue) from AA mice.

**Supplemental Video 2.** Aberrant BM vasculature in SCD mice. 3D-reconstruction of confocal optical sections (LEICA SP8X, 10x objective) of thick femoral slices stained for pan-vasculature marker laminin (green), sinusoid marker endoglin (red), and arteriole/artery marker Sca-1 (blue) from SS mice.

**Supplemental Video 3.** This video shows the flow of transfused CFSE- labeled WT RBCs (green) in an AA control mouse. Time is in seconds. This video is shown at 120 frames/s.

**Supplemental Video 4.** This video shows the flow of transfused CFSE- labeled WT RBCs (green) in a SS mouse. Time is in seconds. This video is shown at 120 frames/s.